

Electronic thermal transport in strongly correlated multilayered nanostructures

J. K. Freericks*

Department of Physics, Georgetown University, Washington, DC 20057-0995

V. Zlatić†

Institute of Physics, Bijenicka c. 46, P. O. B. 304, 1000 Zagreb, Croatia

A. M. Shvaika‡

Institute for Condensed Matter Physics of the National Academy of Sciences of Ukraine, 1 Svientsitskii Street, 79011 Lviv, Ukraine

The formalism for a linear-response many-body treatment of the electronic contributions to thermal transport is developed for multilayered nanostructures. By properly determining the local heat-current operator, it is possible to show that the Jonson-Mahan theorem for the bulk can be extended to inhomogeneous problems, so the various thermal-transport coefficient integrands are related by powers of frequency (including all effects of vertex corrections when appropriate). We illustrate how to use this formalism by showing how it applies to measurements of the Peltier effect, the Seebeck effect, and the thermal conductance.

PACS numbers: 72.15Jf, 72.20Pa, 71.27.+a, 73.21.Ac

I. INTRODUCTION

As materials and device growth techniques mature and improve, it becomes more possible to create artificial systems, composed of well-defined numbers of flat planes of one material grown on top of another material. A device can be engineered by determining the different kinds of materials to grow and the thicknesses of the different multilayers. If we assume the growth process is perfect, so the planes are atomically flat, with no interface roughness, then we have an inhomogeneous quantum-mechanical problem to solve for the behavior of electrons in the system, where the inhomogeneity lies in one dimension only.

The properties of devices grown in this fashion are more complicated if some or all of the materials that make up the device are composed of strongly correlated electron materials, where the properties of the electrons cannot be described solely by an independent-particle picture like band theory. These systems are increasing in interest because bulk strongly correlated materials exhibit exotic phenomena, and show promise in demonstrating high tunability of their properties. What is less studied is how these properties can be modified by confinement/deconfinement effects that are possible in multilayered nanostructures.

In addition, there has been little theoretical development of the thermal transport effects in such multilayered systems. Some evidence from examining the interface between two materials, indicates that thermal transport effects in inhomogeneous systems can create large enhancements to the performance¹, but the theory has not been fully developed within a Kubo-like context which allows the many-body aspects to be treated fully. Semiclassical approaches have also been employed², but that theory is also inadequate to treat strongly correlated materials.

Finally, the important problem of phonon transport in such systems has been examined extensively, but is beyond the scope of what we cover in this work.

One of the most important results in bulk thermal transport is the Jonson-Mahan theorem^{3,4}, which provides an exact relationship between different thermal transport coefficients. Using the Jonson-Mahan theorem makes calculation of the thermal transport only slightly more complicated than the calculation of the charge transport, and has enabled much of the theoretical work in strongly correlated thermoelectrics. Here we show how to generalize the Jonson-Mahan theorem to multilayered nanostructures, which also greatly simplifies the calculation of the thermal transport coefficients.

The idea to use multilayered nanostructures, or more complicated geometries, for enhancing thermoelectric performance of refrigerators or power generators was proposed⁵ in the 1990s and enhancements have been seen recently⁶. The focus in that work was along the ideas of an electron-crystal-phonon-glass approach, where the nanostructures are engineered to preserve the electronic properties, while making the phonon transport similar to that in a disordered glass. It is possible that one can actually employ the nanostructure engineering to produce *enhancements* to the electronic transport properties, while simultaneously reducing the phonon thermal transport, so this basic approach may be pushed further than theorized in the original presentations. One key to being able to enhance the electronic properties, is to be able to tune the electron correlation properties with a proper engineering of the nanostructure and to engineer the charge redistribution at the interfaces. Before initiating such a program, one needs to be able to properly calculate the thermal transport in a strongly correlated device, and we derive the formalism for how to do this here.

The systems we describe in this work involve multilay-

ered devices constructed of atomically flat planes which can be composed of different materials. Each system is inhomogeneous in the z -direction, which is the direction where the planes are stacked. We take the left lead to be identical to the right lead, so the system will have a “mirror symmetry”, and the device will have its chemical potential determined by that of the bulk leads. We use Roman letters (i, j, \dots) to denote the lattice sites within each plane (*i. e.*, the $x - y$ coordinates), and Greek letters (α, β, \dots) to denote the individual planes (*i. e.*, the z -coordinate). We require the system to be translationally invariant within each plane, and for the lattice structure of each plane to be identical, so that the connection between planes is between corresponding sites in the two planes, and is the same for each site. The latter requirement is by no means necessary, but it greatly simplifies the notation for the formalism, so we adopt it here.

We will consider three different types of Hamiltonians here: (i) the Hubbard model⁷; (ii) the Falicov-Kimball model⁸; and (iii) the periodic Anderson model⁹. We use a multiple index αi to denote the i th planar site on plane α . In the Hubbard model, we have conduction electrons, whose creation and annihilation operators are denoted $c_{\alpha i \sigma}^\dagger$ and $c_{\alpha i \sigma}$, respectively, for electrons sitting at the lattice site denoted by αi and with z -component of spin σ . The Falicov-Kimball model has two kinds of electrons: conduction electrons (which are described by similar operators as in the Hubbard model, but without spin, for simplicity) and localized electrons (also chosen to be spinless and created or destroyed by the operators $f_{\alpha i}^\dagger$ and $f_{\alpha i}$). The periodic Anderson model has spin-one-half conduction and f -electrons, which are denoted by the familiar operators, except now all operators will have spin labels. All models can be expressed as the sum of two terms in the Hamiltonian—an inhomogeneous hopping term and an interaction-hybridization term. The inhomogeneous hopping term is essentially the same for all three models. It is

$$\begin{aligned} \mathcal{H}_{\text{hop}} = & - \sum_{\alpha} \sum_{i, j \in \text{plane}} \sum_{\sigma} t_{\alpha i j}^{\parallel} c_{\alpha i \sigma}^\dagger c_{\alpha j \sigma} \\ & - \sum_{\alpha} \sum_{i \in \text{plane}} \sum_{\sigma} t_{\alpha \alpha+1}^{\perp} c_{\alpha i \sigma}^\dagger c_{\alpha+1 i \sigma} \\ & - \sum_{\alpha} \sum_{i \in \text{plane}} \sum_{\sigma} t_{\alpha \alpha+1}^{\perp} c_{\alpha+1 i \sigma}^\dagger c_{\alpha i \sigma} \end{aligned} \quad (1)$$

where we do not include a sum over spin for the spinless Falicov-Kimball model. We assume the hopping matrices are real symmetric matrices, and one should note that the hopping between planes is only between neighboring planes and between corresponding sites within the two planes. The magnitudes of the hopping matrices within the planes and between the planes can vary, but the planar hopping matrices must be translationally invariant to go to a mixed momentum-space-real-space basis, which is commonly done in these types of problems. If the planes are square-lattice planes, then the underlying lattice topology will be that of a simple cubic lattice, but

the hopping need not be the same everywhere.

The interaction-hybridization term is different for each model. For the Hubbard model it is

$$\mathcal{H}_{\text{int}}^{\text{Hub}} = \sum_{\alpha} \sum_{i \in \text{plane}} U_{\alpha} c_{\alpha i \uparrow}^\dagger c_{\alpha i \uparrow} c_{\alpha i \downarrow}^\dagger c_{\alpha i \downarrow}, \quad (2)$$

for the spinless Falicov-Kimball model it is

$$\mathcal{H}_{\text{int}}^{\text{FK}} = \sum_{\alpha} \sum_{i \in \text{plane}} U_{\alpha} c_{\alpha i}^\dagger c_{\alpha i} f_{\alpha i}^\dagger f_{\alpha i}, \quad (3)$$

and for the periodic Anderson model it is

$$\begin{aligned} \mathcal{H}_{\text{int}}^{\text{pam}} = & \sum_{\alpha} \sum_{i \in \text{plane}} \sum_{\sigma} E_{F\alpha} f_{\alpha i \sigma}^\dagger f_{\alpha i \sigma} \\ & + \sum_{\alpha} \sum_{i \in \text{plane}} U_{\alpha} f_{\alpha i \uparrow}^\dagger f_{\alpha i \uparrow} f_{\alpha i \downarrow}^\dagger f_{\alpha i \downarrow} \\ & + \sum_{\alpha} \sum_{i \in \text{plane}} \sum_{\sigma} V_{\alpha}^{\text{hyb}} \left(f_{\alpha i \sigma}^\dagger c_{\alpha i \sigma} + c_{\alpha i \sigma}^\dagger f_{\alpha i \sigma} \right). \end{aligned} \quad (4)$$

For the Falicov-Kimball model, we often replace the term $f_{\alpha i}^\dagger f_{\alpha i}$ by the symbol $w_{\alpha i}$ which equals 0 if no localized electrons are at site αi and equals 1 if a localized electron is at site αi . All interaction and hybridization terms can vary from plane to plane, but they must be the same for every lattice site within the planes to preserve translational invariance within the planes. The total Hamiltonian is then

$$\mathcal{H} = \mathcal{H}_{\text{hop}} + \mathcal{H}_{\text{int}} - \mu \mathcal{N}, \quad (5)$$

for all of the models. The symbol μ is the chemical potential, and \mathcal{N} denotes the electron number operator, chosen to be the total conduction electron number operator for the Hubbard and Falicov-Kimball models and the total electron number operator for the periodic Anderson model (we work in a canonical ensemble for the f -electrons in the Falicov-Kimball model, so no site-energy or chemical potential is needed for those particles).

In Section II, we present a description of electronic charge reconstruction, which naturally occurs in any multilayered device that can be grown for thermoelectric properties. This section briefly reviews the current status of such calculations, and describes their impact on the thermal transport; in particular, it fixes the notation for the internal electrostatic potentials associated with the electronic charge reconstruction. Section III provides the main arguments for developing the multilayered generalization of the Jonson-Mahan theorem. Section IV applies the formalism to three classic experiments—the Peltier effect, the Seebeck effect, and the thermal conductivity. Section V presents our conclusions and describes areas for further work.

II. ELECTRONIC CHARGE RECONSTRUCTION IN MULTILAYERED NANOSTRUCTURES

The Schottky effect¹⁰, is a well-known effect in the semiconductor community, where charge is redistributed between a semiconductor and a metal at a semiconductor-metal interface due to a bulk chemical potential mismatch between the two materials. The charge rearrangement creates a screened dipole layer at the interface resulting in a final state with a static inhomogeneous redistribution of charge through the system. Recently, the phenomenon has been revisited in the context of strongly correlated materials¹¹, where it has been called electronic charge reconstruction^{12,13}. If we imagine a multilayered nanostructure, composed of metallic leads sandwiching a barrier region, which is a strongly correlated material, then the chemical potential of the device is fixed by the chemical potential of the leads. If the chemical potential of the barrier is different, then the system must undergo an electronic charge reconstruction. In particular, since the temperature dependence of the chemical potential should be different in the two different materials, even if the chemical potentials match at one temperature, they will not match at other temperatures, and a charge redistribution will take place.

In this work, we will focus on problems that have “mirror symmetry” for the leads, so the lead to the left is made of the same material as the lead to the right. In this case, the total Coulomb potential energy, due to all electric fields, goes to zero when one is far from the interfaces, because all of the charge rearrangement is localized at the interfaces, and the whole system is charge neutral. If we were to examine systems with different materials for the left and right leads, then the electrochemical potential of the system will be the average of the left and right bulk chemical potentials, which creates some additional complications, but does not change the basic strategies or formulas, although, the Seebeck effect needs to be defined and analyzed with care¹⁴.

The approach to describe the electronic charge reconstruction is a semiclassical one. We solve the problem for local electron interactions exactly, but treat the long-range Coulomb interaction in a mean-field fashion. The strategy we use is to first calculate the electronic charge on each plane via an inhomogeneous Green’s function approach (in dynamical mean-field theory, the technique of Potthoff and Nolting¹⁵ is used). If possible, one uses a Matsubara-frequency approach, because the numerics are usually under better control than real-axis approaches, but this is just a matter of convenience, not necessity. Next, we find the charge deviation on each plane; namely, we determine whether extra charge has entered or left the plane. Since the positive background charge of the ions remains the same, the charge deviation will give rise to an electric field. There are two different ways to treat this field. The simplest is to assume the electric charge is uniformly spread over the plane¹¹. Then the electric

field is constant, perpendicular to the plane, and pointing away from it in both directions if the net charge density is positive, while pointing toward the plane if the net charge density is negative. The second method uses the actual distribution of the ions, and the spatial profile of the electrons, if available, to calculate the charge¹². This approach is closer to an Ewald-like summation¹⁶ of the charge densities. The two treatments should yield similar results.

In this work, we will choose the “constant plane of charge” description for determining the electric fields. This allows us to determine simple analytic expressions for the electric fields—for example, the magnitude of the constant field, emanating from the α th plane of charge is

$$|\mathbf{E}_\alpha| = \frac{|e| |\rho_\alpha - \rho_\alpha^{\text{bulk}}| a}{2\epsilon_0 \epsilon_{r\alpha}}, \quad (6)$$

where $e < 0$ is the charge of the electron, ρ_α is the quantum-mechanically calculated electron number density at plane α , $\rho_\alpha^{\text{bulk}}$ is the bulk electron number density for the material that plane α is composed of (equal to the positive background charge on the plane), ϵ_0 is the permittivity of free space, and $\epsilon_{r\alpha}$ is the relative permittivity of plane α . The contribution to the electric potential $V^c(z)$ from this field satisfies

$$E = -\frac{d}{dz} V^c(z). \quad (7)$$

Since the electric field is constant in magnitude, it is straightforward to compute the contribution to the Coulomb potential at plane β due to the change in the charge density at plane α (but one needs to keep track of the signs of the fields or equivalently the relative order of α with respect to β):

$$V_\beta^c(\alpha) = \frac{|e| (\rho_\alpha - \rho_\alpha^{\text{bulk}}) a}{2\epsilon_0} \times \begin{cases} \sum_{\gamma=\alpha+1}^{\beta} \left[\frac{1}{2\epsilon_{r\gamma}} + \frac{1}{2\epsilon_{r\gamma-1}} \right], & \beta > \alpha \\ 0, & \beta = \alpha \\ \sum_{\gamma=\alpha-1}^{\beta} \left[\frac{1}{2\epsilon_{r\gamma}} + \frac{1}{2\epsilon_{r\gamma+1}} \right], & \beta < \alpha \end{cases} \quad (8)$$

Note that if the relative permittivity ϵ_r is a constant, independent of the planes, then the potential energy is a linear function of the z -coordinate, proportional to $-|\mathbf{z}_\alpha - \mathbf{z}_\beta|/\epsilon_r$ as one might expect. The reason why we need to sum over two terms in the summands in Eq. (8) is because we envision the α th plane of charge to be infinitesimally thick, and go through the lattice sites of plane α , but we assume the dielectric has a thickness of a and is centered around each plane of atoms. Hence, if the permittivity changes from one plane to another, a polarization charge develops halfway between the two planes where the dielectric is changing, and the electric field has a discontinuity at that point (*i. e.*, at the position $\alpha + 1/2$, see Fig. 1).

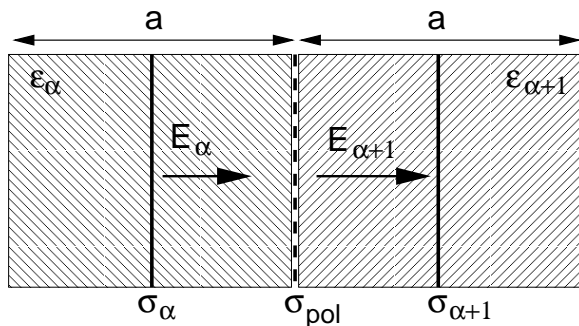


FIG. 1: Geometry taken for the classical electrostatics problem. We show the blow up of two planes, α and $\alpha+1$. Assuming the net surface charge density on plane α is $(\rho_\alpha - \rho_\alpha^{\text{bulk}})a = \sigma_\alpha$ (located along the plane running through position α) and the relative permittivity is $\epsilon_{r\alpha}$ (and similarly for the $\alpha+1$ plane), then the change in polarization at the interface between the two dielectric planes induces a polarization charge on the interface (denoted σ_{pol}) that leads to a discontinuous jump in the electric field halfway between the two lattice planes (at the position $\alpha+1/2$). Once the fields are known, we integrate to get the electric potentials. Note the discontinuity in the electric field occurs at the *midpoint* between the two lattice planes.

It is actually the potential energy $-|e|V_\alpha^c = V_\alpha$ that shifts the chemical potential at each planar site. We define a parameter

$$e_{\text{Schot}}(\alpha) = \frac{e^2 a}{2\epsilon_0 \epsilon_{r\alpha}}, \quad (9)$$

which controls how the extra charge density decays away from the interfaces. The parameter e_{Schot} has the units of an energy multiplied by an area; the product of e_{Schot} with the local density of states has units of the inverse of a length, and this is what determines the decay length of the charge profile. Using this parameter, we can immediately calculate the potential energy due to the Coulomb interaction (evaluated in a mean-field fashion)

$$V_\beta = - \sum_\alpha (\rho_\alpha - \rho_\alpha^{\text{bulk}}) \times \begin{cases} \sum_{\gamma=\alpha+1}^\beta \frac{1}{2} [e_{\text{Schot}}(\gamma) + e_{\text{Schot}}(\gamma-1)], & \beta > \alpha \\ 0, & \beta = \alpha \\ \sum_{\gamma=\alpha-1}^\beta \frac{1}{2} [e_{\text{Schot}}(\gamma) + e_{\text{Schot}}(\gamma+1)], & \beta < \alpha \end{cases}. \quad (10)$$

Note that a similar analysis can be carried out if one uses the Ewald-like technique for determining the charge reconstruction.

These potential energies modify the Hamiltonian by the long-range Coulomb interaction of the charge reconstruction. The additional piece of the Hamiltonian (due to the charge rearrangement) is

$$\mathcal{H}_{\text{charge}} = \sum_\alpha V_\alpha \sum_{i \in \text{plane}} c_{\alpha i}^\dagger c_{\alpha i}. \quad (11)$$

Hence, they can be treated by shifting the chemical potential $\mu \rightarrow \mu - V_\alpha$ on each plane depending on what the Coulomb potential energy is for the given plane. For consistency, we must have that the potentials go to zero as we move far enough into either of the leads (for the mirror-symmetric case). This requirement enforces overall charge conservation—any charge that moves out of the barrier remains in the leads, localized close to the interface, and *vice versa*. Of course, the potentials V_α that appear in the electronic charge reconstruction Hamiltonian in Eq. (11) must be determined self-consistently. Achieving this goal requires care in setting up the iterative algorithm.

There will be no electronic charge reconstruction if the chemical potentials in the bulk of both the leads and the barrier match. In order to have freedom to adjust the mismatch of the chemical potentials, we need to be able to change the value of the band zero of the barrier region relative to the band zero of the leads. This parameter is called $\Delta E_{F\alpha}$, which vanishes in the leads, and is generically a nonzero constant in the barrier (independent of the temperature or the charge rearrangement). Hence we add an additional term

$$\mathcal{H}_{\text{offset}} = - \sum_\alpha \sum_{i \in \text{plane}} \Delta E_{F\alpha} c_{\alpha i}^\dagger c_{\alpha i} \quad (12)$$

to the Hamiltonian. Although this term appears similar to the Coulomb potential term in Eq. (11), the key observation is that this term is fixed and does not change with any parameters of the system, whereas the plane potentials V_α need to be readjusted as the parameters change, to achieve a self-consistent solution of the problem. Note that we set $\Delta E_{F\alpha} = 0$ in the leads to the right and to the left.

In this contribution, we will not discuss how to actually solve for the electronic charge reconstruction in detail. One can imagine a number of different approaches to this problem, ranging from direct means of solving the quantum-mechanical problem on finite-sized stacked planes, to other techniques like the inhomogeneous dynamical mean-field theory approach. The DMFT approach has been quite successful in examining these kinds of problems, and the formalism only requires that the self-energy remain local (although it can vary from plane to plane). Then, by performing a Fourier transform to momentum space for the planar coordinates, one decouples the planar motion from the longitudinal motion. Hence, the problem reduces to a series of quasi-one-dimensional inhomogeneous problems, which can be solved by using the renormalized perturbation expansion¹⁷ (sometimes called the quantum zipper algorithm¹⁸). Details for such an approach have already appeared^{11,18} and are briefly reviewed below.

The DMFT algorithm is given in Fig. 2. If there is a separate algorithm available for the Matsubara frequency Green's functions, then the upper left loop (which determines the electronic charge reconstruction) is used on the imaginary axis, and we don't need it on the real axis. If

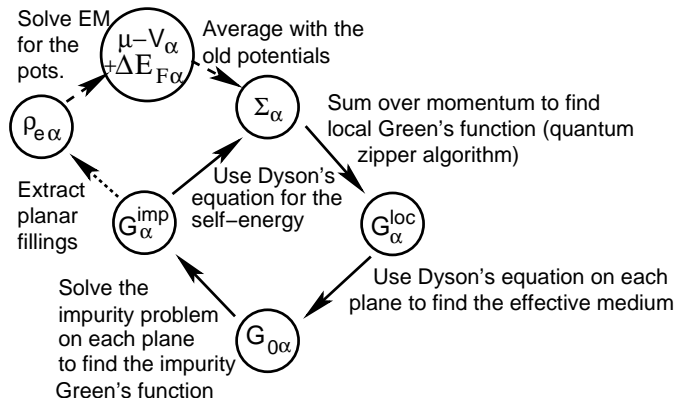


FIG. 2: Flow diagram for the DMFT algorithm in a multilayered nanostructure with electronic charge reconstruction. We determine the charges on each plane, determine how they differ from the bulk charge on the plane to find the excess or deficit charge. Then we use classical electromagnetism to find the electric potentials on each plane and finally the contribution of the potential energy to the electrochemical potential on each plane. Then we average the potentials with a large damping factor so that the potentials are updated slowly. This is then input into the next loop of the main DMFT algorithm, which is unchanged from cases where there is no electronic charge reconstruction.

such an algorithm does not exist (such as when calculations are performed with the numerical renormalization group), then we would use the entire loop on the real axis. The new steps to find the electronic charge reconstruction are to first find the electron density on each plane. Then we subtract the bulk charge density of each plane to find the excess or deficit charge on the given plane. Once the change in charge density is known, we can calculate the electrical potential, and then the contribution to the potential energy. This gets added to the chemical potential to determine the electrochemical potential at each plane.

When numerical results are generated^{11,19} (see those references for numerical issues in the algorithm), we find that usually the electronic charge reconstruction does not change significantly at low temperature, and that the size of the charge deviation grows as the mismatch between the chemical potentials grows (governed in part by the size of $\Delta E_{F\alpha}$ in the barrier). Such results are similar to what one would expect, but most of the calculations have taken place in systems where the charge density is not too sensitive to changes in the chemical potential. The effects may be different in systems with either Mott insulators, or doped Mott insulators, which can be brought close to the insulating phase via the electronic charge reconstruction. In addition, electron-phonon coupled systems can develop a strong sensitivity of the charge to the chemical potential when the coupling is large, which may be an interesting case to examine as well.

Ultimately, we are most interested in the transport of charge and heat through the device. In order to cal-

culate the transport, we need to evaluate the real-axis results for the self-energies and Green's functions of a nanostructure with an electronic charge reconstruction. Unfortunately, the algorithms used when there is no electronic charge reconstruction^{15,18} cannot be simply employed for this case. The reason why is that the presence of the different potentials V_α on each plane causes the nature of the integrands over the two-dimensional density of states to have a different singular behavior than they had before. In a system without electronic charge reconstruction, the singularities in the integrand could be square-root-like, which are removed by a simple variable change using trigonometric or hyperbolic functions. Now, the singularities are poles (because the denominators are shifted by the potentials at a given plane, so they vanish at different energies, and give rise to a different singular behavior), and we need to evaluate all integrals in a principal-value sense, where the real part is integrated with a symmetric grid around each pole, and the imaginary part has a delta-function contribution that needs to be included. This is challenging to implement numerically, because the locations of the poles are different on different planes, and can vary from one iteration to the next. Details for how to deal with such a sophistication will appear elsewhere, since they are beyond the scope of this work.

III. PROOF OF THE INHOMOGENEOUS JONSON-MAHAN THEOREM

It is important to examine how the linear-response transport formalism¹⁸ is modified by the presence of an electronic charge reconstruction. We have taken the chemical potential as a constant throughout the multilayered nanostructure for thermodynamic equilibrium. One can directly show that the device carries no longitudinal charge current even though there are nonzero electric fields arising from the electronic charge reconstruction (see Appendix A for a proof when the self-energy is local). No current flows because the putative current driven by the internal electric fields is canceled by an equal magnitude but oppositely directed current driven by the concentration gradients. The standard way to describe this result is via a phenomenological equation (for the case with no thermal gradients)²⁰

$$\begin{aligned} \langle j^c \rangle &= a \sum_{\beta} \sigma_{\alpha\beta} E_{\beta} - a|e| \sum_{\beta} \mathcal{D}_{\alpha\beta} \frac{\rho_{\beta+1} - \rho_{\beta}}{a} \\ &= -\frac{a}{|e|} \sum_{\beta} \sigma_{\alpha\beta} \frac{\tilde{\mu}_{\beta+1} - \tilde{\mu}_{\beta}}{a}, \end{aligned} \quad (13)$$

where $\mathcal{D}_{\alpha\beta}$ is the diffusion constant for Fick's law of diffusion²¹, and the second equality follows from the Einstein relation²² (or more correctly the Nernst-Einstein-Smoluchowski relation^{23,24}) which relates the diffusion constant to the conductivity via

$$\sigma_{\alpha\beta} = e^2 \mathcal{D}_{\alpha\beta} d\rho_{\beta}/d\mu; \quad (14)$$

both quantities are matrices, with indices given by the planes of the multilayered nanostructure. The symbol $\tilde{\mu}_\alpha = \mu - V_\alpha$ is called the electrochemical potential. The Einstein relation can be derived by relating the gradient with respect to the chemical potential to the gradient with respect to the number concentration via the chain rule: $d\mu/dz = (d\mu/d\rho)d\rho/dz$, and the fact that the current vanishes in equilibrium²⁵.

Eq. (13) implies that the condition for there to be no charge current is simply $d\tilde{\mu}/dz = 0$. The chemical potential is a constant, but it does vary with the filling, so if there is a change in electron concentration, then $d\tilde{\mu}/dz = (d\mu/d\rho)d\rho/dz - dV(z)/dz$, so the force from the electric field will be balanced by the force from the change in electron concentration. In addition, note that the current vanishes no matter how large the variation in the concentration is (*i. e.*, beyond the linear-response regime), so the conclusion is that the current generated by the internal electric field is always canceled by the current generated by the change in the electron concentration. Hence, for a linear-response treatment of transport, we can ignore the forces due to the internal electric fields and the concentration gradients, because they always cancel, and we can limit our focus to the effects of the external electric field only. This then implies that all of the analysis performed previously for the charge current¹⁸ continues to be valid, and because the form of the charge current is unchanged when we have electronic charge reconstruction, the Kubo formula is identical as it was before (with the effects of the potentials V_α included, of course).

The basic observation needed for a thermoelectric device is that there is a difference between the weighting factors that determine the bulk charge current and heat current. The charge current is weighted by the electron velocity, while the heat current is weighted by the velocity multiplied by the kinetic energy minus the chemical potential plus a term from the potential energy. Hence, one can create charge current without heat current, or *vice versa*; by carefully engineering the way electrons move through the device, one can control both the energy and charge flow, which is useful for different types of applications like refrigeration or power generation. A typical device has two legs, one using electrons as the charge carriers and one using holes as the charge carriers. Current flows through the device in a loop, but the net heat flows in one direction only, which allows the device to function.

In this contribution, we concentrate on multilayered nanostructures, which can be used to compose one of the legs of the thermoelectric device. We also concentrate solely on electronic transport mechanisms. In most thermoelectrics, the thermal conductivity from phonons can be large enough to significantly reduce the figure-of-merit. It is expected that the phonon thermal conductivity will be further reduced in a nanostructure, because the interfaces in the nanostructures will cause significant phonon scattering if the masses of the ions in the different materials have a large mismatch⁵, but we do not discuss

this issue further.

There is no simple way to derive the response of a strongly correlated system to both electrical fields and thermal gradients. The reason why is that the thermal gradient cannot be added as a field to the Hamiltonian like the electric field can, hence there is no way to follow the simple Kubo response theory developed for the charge current in an electric field (because the linear-response approach evaluates correlation functions at a fixed temperature, and a variation of the temperature with position is problematic to include within the formalism). Luttinger sorted out a reasonable plan of action for how one can nevertheless proceed²⁵. We couple a fictitious field to the heat-current operator, analogous to the vector potential that couples to the charge current operator, and determine the linear response with respect to both fields. Then, we compare the Kubo response to a phenomenological set of equations that relate the charge and heat currents to the electric field and the gradient of the temperature. We then identify the relevant transport coefficients and how they are expressed in terms of correlation functions.

In multilayered nanostructures, there always is an electronic charge reconstruction, because the bulk chemical potentials for the leads and the barrier will have different T dependence, and hence cannot always be equal (the only exception is for particle-hole symmetry at half-filling, but there the thermopower vanishes, so that case is uninteresting for thermal transport). Hence the Hamiltonian must be modified to include the potential energy V_α on each plane, and the band offsets ΔE_F , as described in Sec. II [*i. e.*, we add $\sum_{\alpha i} (V_\alpha - \Delta E_{F\alpha}) c_{\alpha i}^\dagger c_{\alpha i}$ to \mathcal{H}]. The band offsets are independent of T , and represent the difference in the band zeroes for the leads and the material placed at plane α . The potential energies V_α do depend on T , but they do not create any currents, because they correspond to the static potential associated with the electronic charge reconstruction (and the diffusion current generated by the change in electron concentration cancels the current from the internal electric field; see Appendix A). But the Coulomb potentials do create internal electric fields that maintain the electronic charge redistribution amongst the planes.

The phenomenological study of currents caused by external electric fields or temperature gradients has been examined since the early 1800s. It was found that an electric field can drive a charge current (which is essentially Ohm's law²⁶ with the conductivity as the phenomenological constant) and it can drive a heat current because the electrons carry heat with them as they move through the material (this phenomenon is called the Peltier effect²⁷). Similarly, a temperature gradient can drive heat conduction with the phenomenological thermal conductivity (called Fourier's law²⁸), and because the electronic contribution to the heat current generically carries charge, a temperature gradient can generate a charge current (called the Seebeck effect²⁹). The phenomenological equations for the (linear response) lon-

gitudinal transport in a multilayered nanostructure are then (j_α is the longitudinal number current, j_α^c is the longitudinal charge current, and j_α^Q is the longitudinal heat current)

$$\begin{aligned} \langle j_\alpha^c \rangle &= -|e|\langle j_\alpha \rangle \\ &= |e|a \sum_\beta L_{11\alpha\beta} \left[\frac{d\mu_\beta}{dT} \frac{T_{\beta+1} - T_\beta}{a} + |e|E_\beta \right] \\ &\quad + |e|a \sum_\beta L_{12\alpha\beta} \frac{T_{\beta+1} - T_\beta}{aT_\beta}, \end{aligned} \quad (15)$$

$$\begin{aligned} \langle j_\alpha^Q \rangle &= -a \sum_\beta L_{21\alpha\beta} \left[\frac{d\mu_\beta}{dT} \frac{T_{\beta+1} - T_\beta}{a} + |e|E_\beta \right] \\ &\quad - a \sum_\beta L_{22\alpha\beta} \frac{T_{\beta+1} - T_\beta}{aT_\beta}, \end{aligned} \quad (16)$$

where the indices α and β denote the planar sites (or the midpoint between planar sites, as clarified below), the term $(T_{\beta+1} - T_\beta)/a$ is the discretized approximation to the temperature gradient and the L_{ij} coefficients can be thought of as the phenomenological parameters. We define the symbol $\mu_\beta = \mu - V_\beta + \Delta E_{F\beta}$, which may be thought of as the ‘‘local chemical potential’’ for plane β . The origin of the temperature derivative of μ_β entering into the phenomenological equations arises from the conventional $\nabla\mu$ term, which becomes $\nabla T d\mu/dT$ when the system is placed in a thermal gradient. The spatial derivative of the V_β terms does not drive any current, because it cancels with the current driven by the equilibrium concentration gradient (which we did not include in the above phenomenological equations), so the electric field E_β is the *external field* applied to the device (this is valid only in the linear-response regime of a small external electric field). Note, that there is a simple way to understand the signs that appear in Eqs. (15) and (16). First consider the external electric field, which can be written as the negative gradient of the electric potential. The current (whether of electrons or of holes), always runs down the potential hill. Since the conductivity is always positive, the first term in Eq. (15) must have a positive sign. The thermoelectric number current also runs downhill, so it is proportional to the negative temperature gradient. For electrons, the charge current is $-|e|$ times the number current, which gives rise to the positive sign for the last term in Eq. (15). Similarly, the thermal conductivity runs down the temperature ‘‘hill’’, so it has a negative sign in front of it. The Peltier effect term is the hardest to understand, but because the electrons are negatively charged, they actually move up the potential hill (the charge current runs down the hill because the electrons are negatively charged), so the heat is carried up the hill, and hence there is a minus sign in front of the term (recall the electric field is the negative gradient of the potential).

Our next step is to determine how to represent the thermal transport coefficients L_{ij} in terms of many-body

correlation functions. This has already been done for the first coefficient¹⁸, which is proportional to the conductivity matrix, and is represented by a current-current correlation function: $\sigma_{\alpha\beta} = e^2 L_{11\alpha\beta}$ (the modification of the Hamiltonian by the electronic charge reconstruction has no effect on the form of the charge current, or on the form of the correlations functions, but obviously creates additional scattering). Since this coefficient arises from an electric field, which can be added to the Hamiltonian, the derivation is rigorous. Similarly, if we follow all the steps in Ref. 18 that led up to the derivation of the conductivity matrix, but we examined the expectation value of the heat-current operator instead of the charge-current operator, we would find that the L_{21} correlation function was identical to the L_{11} correlation function except that it is a heat-current–charge-current correlation function instead of a charge-current–charge-current correlation function.

As we discussed above, there is no complete theory to determine the L_{12} and L_{22} coefficients for the phenomenological transport equations. But, classical nonequilibrium statistical mechanics has proved that there is a reciprocal relation between the ‘‘cross’’ terms in the transport equations²⁰. Written in the form we have them, this relation says that $L_{21} = L_{12}$. Knowing the form for L_{21} , we then conclude that L_{12} is the charge-current–heat-current correlation function. Keeping within this same vein, the natural conclusion is that the final transport coefficient L_{22} is a heat-current–heat-current correlation function (but there is no rigorous derivation of this result).

In order to derive the local charge and heat current operators, we must formulate the transport problem in real space. Unlike the bulk case, where the procedure is completely well-defined, there are a number of different possible ways to try to derive the local current operators. The bulk number current operator is found by taking the commutator of the number polarization operator with the Hamiltonian; this guarantees that the equation of continuity holds, and it also implies that the number current is conserved through the system. The number polarization operator is

$$\Pi^{\text{number}} = \sum_{\alpha i} \mathbf{R}_{\alpha i} (c_{\alpha i}^\dagger c_{\alpha i} + f_{\alpha i}^\dagger f_{\alpha i}), \quad (17)$$

where we dropped the spin index for simplicity, and where $\mathbf{R}_{\alpha i}$ is the position vector of the site labeled by αi . The $f^\dagger f$ term enters for the Falicov-Kimball and periodic Anderson models, but not for the Hubbard model. Since the number polarization operator depends only on the number operators, it commutes with all number operators in the interaction Hamiltonian. It turns out that the form in Eq. (17) also commutes with the hybridization term in the periodic Anderson model because the hybridization is on-site only. Hence, the bulk number current operator is the same for all models we examine here, and arises solely from the commutator of the z -component of the polarization operator with the hopping

Hamiltonian. Performing the commutator is straightforward, and leads to $j = \sum_{\alpha} j_{\alpha}$, with

$$j_{\alpha} = -iat_{\alpha\alpha+1}^{\perp} \sum_{i \in \text{plane}} \left(c_{\alpha i}^{\dagger} c_{\alpha+1 i} - c_{\alpha+1 i}^{\dagger} c_{\alpha i} \right). \quad (18)$$

Note that the subscript α on the current operator denotes the total current operator flowing through the α th plane, and does not indicate a Cartesian coordinate of the current operator; the current operator is always taken in the z -direction for the longitudinal flow. The current at plane α is thus defined to be the total number of electrons flowing to the left minus the total flowing to the right (here the current operator at plane α is determined by the number of electrons flowing to the right or to the left through the α th and $\alpha + 1$ st planes).

A comment is in order about the choice given in Eq. (18) for the current associated with the α th plane. Note that the form chosen is not the same as the choice that would arise from taking the commutator of the “local” polarization operator (at the α th plane) with the Hamiltonian. The direct result from the commutator $\hat{j}_{\alpha} = i[\mathcal{H}, \sum_{i \in \text{plane}} z_{\alpha} (c_{\alpha i}^{\dagger} c_{\alpha i} + f_{\alpha i}^{\dagger} f_{\alpha i})]$

$$\begin{aligned} \hat{j}_{\alpha} &= -i \sum_{i \in \text{plane}} [t_{\alpha\alpha+1}^{\perp} (c_{\alpha+1 i}^{\dagger} c_{\alpha i} - c_{\alpha i}^{\dagger} c_{\alpha+1 i}) \\ &\quad + t_{\alpha-1\alpha}^{\perp} (c_{\alpha-1 i}^{\dagger} c_{\alpha i} - c_{\alpha i}^{\dagger} c_{\alpha-1 i})] z_{\alpha}, \end{aligned} \quad (19)$$

does not seem reasonable, because it is weighted by the z -coordinate of the α th plane, rather than involving the difference of currents moving in opposite directions (at the α th plane). When we have full translational symmetry, we derive the conventional form for the current operator by shifting the spatial index of one of the terms, to explicitly carry out the cancellation of the spatial coordinates (just take the summation of the above result over α , and shift $\alpha \rightarrow \alpha + 1$ in the last two terms). More reflection on this issue, shows that the explicit form of the local current operator that enters the Kubo formula actually originates from the coupling term $-\mathbf{j} \cdot \mathbf{A}$ term that corresponds to the perturbation of the Hamiltonian due to the electric field in a gauge where the scalar potential vanishes; this is because we evaluate the expectation value of the total current with the perturbation of the Hamiltonian due to the external field and that field enters via the vector potential value at a specific plane. Hence the conductivity matrix is defined from the piece of the total current operator that couples to the field at plane α and, since the total current will be the sum of the currents at each plane, the current-current correlation function for the conductivity matrix involves the local current operators that couple to the vector potential. Thus, we choose the perturbation of the Hamiltonian to be

$$\mathcal{H}'(t) = -ie|a \sum_{\alpha i} t_{\alpha\alpha+1}^{\perp} (c_{\alpha+1 i}^{\dagger} c_{\alpha i} - c_{\alpha i}^{\dagger} c_{\alpha+1 i}) A_{\alpha}(t), \quad (20)$$

where we have taken the vector potential along the z -direction, and independent of the intraplane coordinates,

because the field is uniform for each plane. We feel this choice makes good physical sense because we couple the vector potential to the physical current between the α th and $\alpha + 1$ st planes. Alternatively, one can view this as a coupling of the current between the α th and $\alpha + 1$ st plane to the electric vector potential located halfway between those two planes (in this interpretation, we would use $[A_{\alpha} + A_{\alpha+1}]/2$ as the coupling field). Finally, one can take a symmetrized version of the local current operator to be

$$\begin{aligned} j_{\alpha}^{\text{sym}} &= -iat_{\alpha-1\alpha}^{\perp} \sum_{i \in \text{plane}} (c_{\alpha i}^{\dagger} c_{\alpha-1 i} - c_{\alpha-1 i}^{\dagger} c_{\alpha i})/2 \\ &\quad - iat_{\alpha\alpha+1}^{\perp} \sum_{i \in \text{plane}} (c_{\alpha+1 i}^{\dagger} c_{\alpha i} - c_{\alpha i}^{\dagger} c_{\alpha+1 i})/2, \end{aligned} \quad (21)$$

corresponding to the average of the currents located just to the left and to the right of plane α . This choice sounds like the most physical choice, but the calculations for it are somewhat more complicated, and it is not likely the end results are too different from our first choice. The difference between the two choices is actually quite simple. In the first approach, one should envision the spatial indices α and β to correspond to $z_{\alpha} + a/2$ and $z_{\beta} + a/2$; that is, they are shifted to the right by half the distance between the planes. In the second, symmetrized approach, the α and β indices denote the planar indices. For this reason, we don't expect the final results to be too different for either approach. For simplicity, we choose to take the current operator to be the current between the α th and $\alpha + 1$ st planes for our derivations below, and we discuss how to get the corresponding symmetrized results at the end.

The calculation of the local heat current operator is more complicated. We adopt the same strategy as before though—first calculate the bulk operator, and then extract a reasonable choice for the local operator. To calculate the bulk heat current operator, we first need to determine the energy polarization operator. This is similar to the number polarization operator, except it is weighted by the piece of the Hamiltonian associated with the αi position. This is easy to do for the interaction and hybridization terms, the Coulomb potential energy terms, and the band offset terms, which are local, but is complicated for the hopping terms, which involve two lattice sites. The procedure that is used is to associate half of the hopping term between the two sites with the local Hamiltonian at each of those two sites. The energy polarization term then becomes

$$\begin{aligned} \Pi^E &= \sum_{\alpha} \sum_{i \in \text{plane}} \left[\frac{1}{2} \sum_{\beta} \sum_{j \in \text{plane}} \mathcal{H}_{\text{hop } \alpha i \beta j} + \mathcal{H}_{\text{int } \alpha i} \right. \\ &\quad \left. + \mathcal{H}_{\text{charge } \alpha i} + \mathcal{H}_{\text{offset } \alpha i} \right] \mathbf{R}_{\alpha i}, \end{aligned} \quad (22)$$

where the hopping piece is divided into two as described above, and the interaction piece includes all the local parts of the interacting Hamiltonian associated with each

lattice site. The bulk energy current operator is $j^E = i[\mathcal{H}, \Pi^E]$, and the heat-current operator is $j^Q = j^E - \mu j$ because the heat is the energy measured relative to the chemical potential. The commutator is tedious to work out, but just involves straightforward algebra. When it is finished, we have an expression for the bulk heat current, which can be organized into summations that involve a plane α and the plane to the right (there is also a hopping term involving operators at the $\alpha + 2$ plane). One simply

groups the terms together to find how to make an educated guess for the local heat current operator. The final results that we have are summarized below. These are the proper local heat current operators needed to satisfy the Jonsen-Mahan theorem, as described below. In all cases, we have $j^Q = \sum_{\alpha} j_{\alpha}^Q$. Note that we can form the symmetric version of the heat current operator as well, if desired, but it is even more complex.

For the Hubbard model, we have

$$\begin{aligned} \mathbf{j}_{\alpha}^Q &= iat_{\alpha\alpha+1}^{\perp} \left\{ - \sum_{ij \in \text{plane}, \sigma} \frac{1}{2} (t_{\alpha ij}^{\parallel} + t_{\alpha+1 ij}^{\parallel}) (c_{\alpha+1 i \sigma}^{\dagger} c_{\alpha j \sigma} - c_{\alpha i \sigma}^{\dagger} c_{\alpha+1 j \sigma}) \right. \\ &\quad - \frac{1}{2} t_{\alpha+1 \alpha+2}^{\perp} \sum_{i \in \text{plane}, \sigma} (c_{\alpha+2 i \sigma}^{\dagger} c_{\alpha i \sigma} - c_{\alpha i \sigma}^{\dagger} c_{\alpha+2 i \sigma}) - \frac{1}{2} t_{\alpha-1 \alpha}^{\perp} \sum_{i \in \text{plane}, \sigma} (c_{\alpha+1 i \sigma}^{\dagger} c_{\alpha-1 i \sigma} - c_{\alpha-1 i \sigma}^{\dagger} c_{\alpha+1 i \sigma}) \\ &\quad + \sum_{i \in \text{plane}, \sigma} \left[-\mu + \frac{1}{2} (V_{\alpha} + V_{\alpha+1}) - \frac{1}{2} (\Delta E_{F\alpha} + \Delta E_{F\alpha+1}) \right] (c_{\alpha+1 i \sigma}^{\dagger} c_{\alpha i \sigma} - c_{\alpha i \sigma}^{\dagger} c_{\alpha+1 i \sigma}) \\ &\quad \left. + \frac{1}{2} \sum_{i \in \text{plane}, \sigma} (U_{\alpha} c_{\alpha i \bar{\sigma}}^{\dagger} c_{\alpha i \bar{\sigma}} + U_{\alpha+1} c_{\alpha+1 i \bar{\sigma}}^{\dagger} c_{\alpha+1 i \bar{\sigma}}) (c_{\alpha+1 i \sigma}^{\dagger} c_{\alpha i \sigma} - c_{\alpha i \sigma}^{\dagger} c_{\alpha+1 i \sigma}) \right\}, \end{aligned} \quad (23)$$

where $\bar{\sigma} = -\sigma$ denotes the spin state opposite to σ . For the Falicov-Kimball model, we find

$$\begin{aligned} \mathbf{j}_{\alpha}^Q &= iat_{\alpha\alpha+1}^{\perp} \left\{ - \sum_{ij \in \text{plane}} \frac{1}{2} (t_{\alpha ij}^{\parallel} + t_{\alpha+1 ij}^{\parallel}) (c_{\alpha+1 i}^{\dagger} c_{\alpha j} - c_{\alpha i}^{\dagger} c_{\alpha+1 j}) - \frac{1}{2} t_{\alpha+1 \alpha+2}^{\perp} \sum_{i \in \text{plane}} (c_{\alpha+2 i}^{\dagger} c_{\alpha i} - c_{\alpha i}^{\dagger} c_{\alpha+2 i}) \right. \\ &\quad - \frac{1}{2} t_{\alpha-1 \alpha}^{\perp} \sum_{i \in \text{plane}} (c_{\alpha+1 i}^{\dagger} c_{\alpha-1 i} - c_{\alpha-1 i}^{\dagger} c_{\alpha+1 i}) + \frac{1}{2} \sum_{i \in \text{plane}} (U_{\alpha} w_{\alpha i} + U_{\alpha+1} w_{\alpha+1 i}) (c_{\alpha+1 i}^{\dagger} c_{\alpha i} - c_{\alpha i}^{\dagger} c_{\alpha+1 i}) \\ &\quad \left. + \sum_{i \in \text{plane}} \left[-\mu + \frac{1}{2} (V_{\alpha} + V_{\alpha+1}) - \frac{1}{2} (\Delta E_{F\alpha} + \Delta E_{F\alpha+1}) \right] (c_{\alpha+1 i}^{\dagger} c_{\alpha i} - c_{\alpha i}^{\dagger} c_{\alpha+1 i}) \right\}. \end{aligned} \quad (24)$$

For the periodic Anderson model the commutation of the Hamiltonian with the energy polarization operator gives

$$\begin{aligned} \mathbf{j}_{\alpha}^Q &= iat_{\alpha\alpha+1}^{\perp} \left\{ - \sum_{ij \in \text{plane}, \sigma} \frac{1}{2} (t_{\alpha ij}^{\parallel} + t_{\alpha+1 ij}^{\parallel}) (c_{\alpha+1 i \sigma}^{\dagger} c_{\alpha j \sigma} - c_{\alpha i \sigma}^{\dagger} c_{\alpha+1 j \sigma}) \right. \\ &\quad - \frac{1}{2} t_{\alpha+1 \alpha+2}^{\perp} \sum_{i \in \text{plane}, \sigma} (c_{\alpha+2 i \sigma}^{\dagger} c_{\alpha i \sigma} - c_{\alpha i \sigma}^{\dagger} c_{\alpha+2 i \sigma}) - \frac{1}{2} t_{\alpha-1 \alpha}^{\perp} \sum_{i \in \text{plane}, \sigma} (c_{\alpha+1 i \sigma}^{\dagger} c_{\alpha-1 i \sigma} - c_{\alpha-1 i \sigma}^{\dagger} c_{\alpha+1 i \sigma}) \\ &\quad \left. + \sum_{i \in \text{plane}, \sigma} \left[-\mu + \frac{1}{2} (V_{\alpha} + V_{\alpha+1}) - \frac{1}{2} (\Delta E_{F\alpha} + \Delta E_{F\alpha+1}) \right] (c_{\alpha+1 i \sigma}^{\dagger} c_{\alpha i \sigma} - c_{\alpha i \sigma}^{\dagger} c_{\alpha+1 i \sigma}) \right\} \\ &\quad + iaV_{\alpha}^{hyb} \frac{1}{2} \sum_{i \in \text{plane}, \sigma} \left[t_{\alpha\alpha+1}^{\perp} (f_{\alpha i \sigma}^{\dagger} c_{\alpha+1 i \sigma} - c_{\alpha+1 i \sigma}^{\dagger} f_{\alpha i \sigma}) + t_{\alpha\alpha-1}^{\perp} (f_{\alpha i \sigma}^{\dagger} c_{\alpha-1 i \sigma} - c_{\alpha-1 i \sigma}^{\dagger} f_{\alpha i \sigma}) \right] \\ &\quad + iat_{\alpha\alpha+1}^{\perp} \frac{1}{2} \sum_{i \in \text{plane}, \sigma} \left[(U_{\alpha} f_{\alpha i \bar{\sigma}}^{\dagger} f_{\alpha i \bar{\sigma}} + U_{\alpha+1} f_{\alpha+1 i \bar{\sigma}}^{\dagger} f_{\alpha+1 i \bar{\sigma}}) (f_{\alpha+1 i \sigma}^{\dagger} f_{\alpha i \sigma} - f_{\alpha i \sigma}^{\dagger} f_{\alpha+1 i \sigma}) \right]. \end{aligned} \quad (25)$$

The heat current operator depends on the model being examined, because it involves commutators of the potential energy with the energy polarization. We also sub-

tract the chemical potential multiplied by the number current from the energy current to get the heat current. One might have thought we should subtract the “local

chemical potential” multiplied by the local number current operator, but that would remove the extra terms in the heat current arising from the electronic charge reconstruction; one could have grouped those terms into either the Hamiltonian or the local chemical potential—we chose the former, so we subtract only μj .

Now we need to determine the dc limit of the correlation functions L_{ij} on the real axis. The analytic-continuation procedure is identical to that for the bulk case. We start by defining a polarization operator on the imaginary axis, then we analytically continue to the real axis, we form the relevant transport coefficient, and then we take the limit of the frequency going to zero. We denote four polarization operators by $\bar{L}_{ij\alpha\beta}(i\nu)$ according to

$$\begin{aligned}\bar{L}_{11\alpha\beta}(i\nu) &= \int_0^\beta d\tau e^{i\nu\tau} \langle \mathcal{T}_\tau j_\alpha(\tau) j_\beta(0) \rangle, \\ \bar{L}_{12\alpha\beta}(i\nu) &= \int_0^\beta d\tau e^{i\nu\tau} \langle \mathcal{T}_\tau j_\alpha(\tau) j_\beta^Q(0) \rangle, \\ \bar{L}_{21\alpha\beta}(i\nu) &= \int_0^\beta d\tau e^{i\nu\tau} \langle \mathcal{T}_\tau j_\alpha^Q(\tau) j_\beta(0) \rangle, \\ \bar{L}_{22\alpha\beta}(i\nu) &= \int_0^\beta d\tau e^{i\nu\tau} \langle \mathcal{T}_\tau j_\alpha^Q(\tau) j_\beta^Q(0) \rangle,\end{aligned}\quad (26)$$

and the transport coefficients satisfy

$$\begin{aligned}L_{ij\alpha\beta} &= \lim_{\nu \rightarrow 0} \frac{1}{2i\nu} [\bar{L}_{ij\alpha\beta}(\nu + i0^+) - \bar{L}_{ij\alpha\beta}(\nu + i0^-)] \\ &= \lim_{\nu \rightarrow 0} \text{Re}[-i\bar{L}_{ij\alpha\beta}(\nu)/\nu]\end{aligned}\quad (27)$$

(the ij subscripts here are 1 or 2, and not the planar site indices). The generic notation $\mathcal{O}(\tau) = \exp[(\mathcal{H} - \mu\mathcal{N})\tau]\mathcal{O}\exp[-(\mathcal{H} - \mu\mathcal{N})\tau]$ is used to indicate the time dependence of the operators in Eq. (26). The Jonsen-Mahan theorem^{3,4} can be straightforwardly generalized to treat this case. Begin by defining a generalized function

$$\begin{aligned}F_{\alpha\beta}(\tau_1, \tau_2, \tau_3, \tau_4) &= \left\langle \mathcal{T}_\tau iat_{\alpha\alpha+1}^\perp \sum_{i \in \text{plane}} \left[c_{\alpha+1i}^\dagger(\tau_1) c_{\alpha i}(\tau_2) - c_{\alpha i}^\dagger(\tau_1) c_{\alpha+1i}(\tau_2) \right] \right. \\ &\quad \left. \times iat_{\beta\beta+1}^\perp \sum_{j \in \text{plane}} \left[c_{\beta+1j}^\dagger(\tau_3) c_{\beta j}(\tau_4) - c_{\beta j}^\dagger(\tau_3) c_{\beta+1j}(\tau_4) \right] \right\rangle.\end{aligned}\quad (28)$$

Next, we determine the polarization operators by taking the appropriate limits and derivatives. Namely,

$$\begin{aligned}\bar{L}_{11\alpha\beta}(i\nu) &= \int_0^\beta d\tau_1 e^{i\nu\tau_1} F_{\alpha\beta}(\tau_1, \tau_1^-, 0, 0^-), \\ \bar{L}_{12\alpha\beta}(i\nu) &= \int_0^\beta d\tau_1 e^{i\nu\tau_1} \frac{1}{2} \left(\frac{\partial}{\partial\tau_3} - \frac{\partial}{\partial\tau_4} \right) F_{\alpha\beta}(\tau_1, \tau_1^-, \tau_3, \tau_4) \Big|_{\tau_3=0, \tau_4=0^-}, \\ \bar{L}_{21\alpha\beta}(i\nu) &= \int_0^\beta d\tau_1 e^{i\nu\tau_1} \frac{1}{2} \left(\frac{\partial}{\partial\tau_1} - \frac{\partial}{\partial\tau_2} \right) F_{\alpha\beta}(\tau_1, \tau_2, 0, 0^-) \Big|_{\tau_2=\tau_1^-}, \\ \bar{L}_{22\alpha\beta}(i\nu) &= \int_0^\beta d\tau_1 e^{i\nu\tau_1} \frac{1}{4} \left(\frac{\partial}{\partial\tau_1} - \frac{\partial}{\partial\tau_2} \right) \left(\frac{\partial}{\partial\tau_3} - \frac{\partial}{\partial\tau_4} \right) F_{\alpha\beta}(\tau_1, \tau_2, \tau_3, \tau_4) \Big|_{\tau_2=\tau_1^-, \tau_3=0, \tau_4=0^-}.\end{aligned}\quad (29)$$

This result holds because the $(\partial_\tau - \partial_{\tau'})/2$ operator converts the local number current operator into the local heat current operator. To see this, we simply compute

$$\begin{aligned}&\lim_{\tau' \rightarrow \tau} \frac{1}{2} \left(\frac{\partial}{\partial\tau} - \frac{\partial}{\partial\tau'} \right) iat_{\alpha\alpha+1}^\perp \sum_{i \in \text{plane}} \left[c_{\alpha+1i}^\dagger(\tau) c_{\alpha i}(\tau') - c_{\alpha i}^\dagger(\tau) c_{\alpha+1i}(\tau') \right] \\ &= iat_{\alpha\alpha+1}^\perp \sum_{i \in \text{plane}} \left\{ [\mathcal{H} - \mu\mathcal{N}, c_{\alpha+1i}^\dagger(\tau)] c_{\alpha i}(\tau) + c_{\alpha+1i}^\dagger(\tau) [\mathcal{H} - \mu\mathcal{N}, c_{\alpha i}(\tau)] \right\},\end{aligned}\quad (30)$$

which can be shown to be equal to j_α^Q when the commuta-

tors are evaluated. It is this critical identity that connects

the local number and heat current operators that is a requirement for the formalism to satisfy the Jonson-Mahan theorem. The analytic continuation is complex, because it involves four-time functions in the general case, and a detailed proof of the Jonson-Mahan theorem appears in Appendix B. Instead, we provide a direct constructive proof in DMFT here, where we neglect the vertex corrections. This is just a heuristic approach to the full problem.

The first step is to evaluate the expectation values of the Fermionic operators (in the definition of F) via contractions, because we neglect the vertex corrections. This yields

$$\begin{aligned} F_{\alpha\beta}(\tau_1, \tau_2, \tau_3, \tau_4) &= a^2 t_{\alpha\alpha+1} t_{\beta\beta+1} \\ &\sum_{ij \in \text{plane}} \{ G_{\beta\alpha+1ji}(\tau_4 - \tau_1) G_{\alpha\beta+1ij}(\tau_2 - \tau_3) \\ &- G_{\beta+1\alpha+1ji}(\tau_4 - \tau_1) G_{\alpha\beta ij}(\tau_2 - \tau_3) \\ &- G_{\beta\alpha ji}(\tau_4 - \tau_1) G_{\alpha+1\beta+1ij}(\tau_2 - \tau_3) \\ &+ G_{\beta+1\alpha ji}(\tau_4 - \tau_1) G_{\alpha+1\beta ij}(\tau_2 - \tau_3) \}. \end{aligned} \quad (31)$$

Next, we need to determine a spectral representation for the off-diagonal Green's function. Using the fact that

$$G_{\alpha\beta ij}(z) = -\frac{1}{\pi} \int d\omega \frac{\text{Im} G_{\alpha\beta ij}(\omega)}{z - \omega}, \quad (32)$$

with z in the upper half plane (which can be shown by using the Lehmann representation), says that

$$G_{\alpha\beta ij}(\tau) = -\frac{1}{\pi} \int d\omega T \sum_n \frac{e^{-i\omega_n \tau}}{i\omega_n - \omega} \text{Im} G_{\alpha\beta ij}(\omega). \quad (33)$$

Now we convert the sum over Matsubara frequencies into a contour integral (that surrounds each Matsubara frequency, but does not cross the real axis—the contour is then deformed into two contours, one running just above and the other just below the real axis), but we must be careful to ensure that the procedure is well-defined. If $\tau < 0$, then

$$\begin{aligned} T \sum_n \frac{e^{-i\omega_n \tau}}{i\omega_n - \omega} &= -\frac{i}{2\pi} \int_C dz \frac{e^{-z\tau}}{z - \omega} f(z), \\ &= -\frac{i}{2\pi} \int_{-\infty}^{\infty} dz e^{-z\tau} f(z) \\ &\quad \left[\frac{1}{z + i0^+ - \omega} - \frac{1}{z - i0^+ - \omega} \right], \\ &= -e^{-\omega\tau} f(\omega). \end{aligned} \quad (34)$$

This result is well-defined because the Fermi factor provides convergence (asymptotically like $\exp[-\beta z]$) for $z \rightarrow \infty$ and the $\exp[-z\tau]$ term provides boundedness for $z \rightarrow -\infty$ when $\tau < 0$. Since $1 - f(z)$ has the same poles as $f(z)$ on the imaginary axis, with residues that have the opposite sign, and it behaves like $\exp[\beta z]$ for $z \rightarrow -\infty$, one finds

$$T \sum_n \frac{e^{-i\omega_n \tau}}{i\omega_n - \omega} = e^{-\omega\tau} [1 - f(\omega)], \quad (35)$$

for $\tau > 0$. The results in Eqs. (34) and (35) can then be substituted into Eq. (33) to get the final formula for the off-diagonal Green's function

$$G_{\alpha\beta ij}(\tau) = \begin{cases} -\frac{1}{\pi} \int d\omega \text{Im} G_{\alpha\beta ij}(\omega) e^{-\omega\tau} [1 - f(\omega)], & \tau > 0 \\ -\frac{1}{\pi} \int d\omega \text{Im} G_{\alpha\beta ij}(\omega) e^{-\omega\tau} [-f(\omega)], & \tau < 0. \end{cases} \quad (36)$$

Now we note that we can restrict ourselves to the case $\tau_1 > \tau_2 > \tau_3 > \tau_4$ without loss of generality, because that is the ordering needed to get the relevant correlation functions. Then we employ Eq. (36) in Eq. (31) and use the fact that the summations over the spatial indices for the planes can be Fourier transformed, and then the momentum summation can be replaced by an integration over the two-dimensional density of states, to yield

$$\begin{aligned} F_{\alpha\beta}(\tau_1, \tau_2, \tau_3, \tau_4) &= \frac{a^2}{\pi^2} t_{\alpha\alpha+1}^\perp t_{\beta\beta+1}^\perp \\ &\int d\omega \int d\omega' \int d\epsilon^\parallel \rho^{2d}(\epsilon^\parallel) \\ &\times f(\omega) [1 - f(\omega')] e^{-\omega(\tau_4 - \tau_1) - \omega'(\tau_2 - \tau_3)} \\ &\times \left\{ \text{Im} G_{\beta\alpha}(\epsilon^\parallel, \omega) \text{Im} G_{\alpha+1\beta+1}(\epsilon^\parallel, \omega') \right. \\ &+ \text{Im} G_{\beta+1\alpha+1}(\epsilon^\parallel, \omega) \text{Im} G_{\alpha\beta}(\epsilon^\parallel, \omega') \\ &- \text{Im} G_{\beta\alpha+1}(\epsilon^\parallel, \omega) \text{Im} G_{\alpha\beta+1}(\epsilon^\parallel, \omega') \\ &\left. - \text{Im} G_{\beta+1\alpha}(\epsilon^\parallel, \omega) \text{Im} G_{\alpha+1\beta}(\epsilon^\parallel, \omega') \right\}. \end{aligned} \quad (37)$$

Now we can evaluate the polarizations, and directly perform the analytic continuation. We Fourier transform the expression in Eq. (37) to get the Matsubara frequency representation. Then we replace $i\nu_l$ by $\nu + i0^+$, we construct the transport coefficients on the real axis, and we finally take the limit $\nu \rightarrow 0$ to get the dc response. The factor $(\partial_\tau - \partial_{\tau'})/2$ gives a factor of $(\omega + \omega')/2$ which goes to $(\omega + \nu/2)$ after integrating over the delta function that arises in the analytic continuation. Setting $\nu = 0$ gives an extra power of ω in the integrand for each derivative factor in the response coefficient. The end result is

$$\begin{aligned} L_{ij\alpha\beta} &= \frac{a^2}{\pi} t_{\alpha\alpha+1}^\perp t_{\beta\beta+1}^\perp \int d\omega \left(-\frac{df(\omega)}{d\omega} \right) \omega^{i+j-2} \\ &\int d\epsilon^\parallel \rho^{2d}(\epsilon^\parallel) \\ &\left\{ \text{Im} G_{\beta\alpha}(\epsilon^\parallel, \omega) \text{Im} G_{\alpha+1\beta+1}(\epsilon^\parallel, \omega) \right. \\ &+ \text{Im} G_{\alpha\beta}(\epsilon^\parallel, \omega) \text{Im} G_{\beta+1\alpha+1}(\epsilon^\parallel, \omega) \\ &- \text{Im} G_{\beta\alpha+1}(\epsilon^\parallel, \omega) \text{Im} G_{\alpha\beta+1}(\epsilon^\parallel, \omega) \\ &\left. - \text{Im} G_{\alpha+1\beta}(\epsilon^\parallel, \omega) \text{Im} G_{\beta+1\alpha}(\epsilon^\parallel, \omega) \right\}. \end{aligned} \quad (38)$$

This is the generalized Jonson-Mahan theorem for inhomogeneous systems described by DMFT with vertex corrections neglected. Note that the equality of L_{12} with L_{21} is the Onsager reciprocal relation²⁰.

If one wants to work with symmetrized currents rather than the currents between the α and $\alpha + 1$ st planes, then the Kubo formulas will be changed slightly to take into

account the symmetrized current operators. These can be constructed directly from the correlation functions already illustrated above, and it is a simple exercise to take care of the relevant bookkeeping; we leave such details to the reader.

IV. ANALYSIS OF EXPERIMENTS

With the expressions for the phenomenological coefficients that appear in Eqs. (15) and (16) determined, we now can move onto evaluating the transport in different cases of interest. The first point that needs to be emphasized is that the total number of electrons is always conserved in the system, so the charge current is conserved, and cannot change from plane to plane $\langle j_\alpha^c \rangle = \langle j_\beta^c \rangle$. There is no such conservation law for the heat current though, because the electrons can change the amount of heat that they carry depending on their local environment. Hence, it is the boundary conditions that we impose upon the heat current that determines how it behaves in a multilayered nanostructure. This point will become important as we analyze different experimental situations.

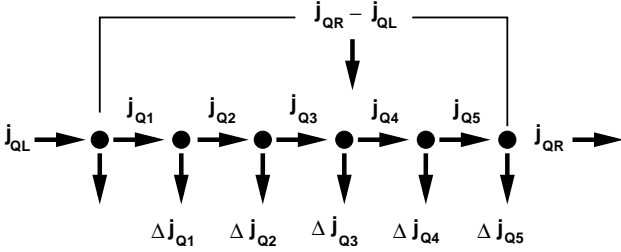


FIG. 3: Schematic diagram of the heat transfers in the Peltier effect. The dots refer to different planes. A heat current is incident from the left. As we go from one plane to another, the heat current changes, as heat is transferred to or from a reservoir to maintain the system at a constant temperature. For example, we can examine the total heat current transferred to the reservoirs ($j_{QR} - j_{QL}$), or we can examine the average heat current that flows through the device $\sum_\alpha j_{Q\alpha}/N$, where N is the number of planes involved in the heat transfer.

The first experiment we would like to analyze is the Peltier effect in a multilayered nanostructure. We imagine that the nanostructure is attached to a bath that maintains the entire structure at a fixed temperature, and we then turn on an external electric field. The Peltier effect is the ratio of the heat current to the charge current. A moment's reflection will show that the heat current is not necessarily conserved in this system, because we have to exchange heat with the reservoir to maintain a constant temperature profile. Hence, it isn't even obvious what ratio should be taken for the Peltier effect—the average heat current for the entire device over the charge current, the total change in the heat current over the charge current, or the heat current transferred to the

reservoir over the charge current. We now show how to determine all three of these results.

The starting point is the transport equations [(15) and (16)] with $T_\alpha = T$ independent of the plane number. We first determine the electric field by multiplying both sides of Eq. (15) by the inverse L_{11} matrix. Since the charge current is independent of the plane index, we find the electric field satisfies

$$E_\alpha = \frac{1}{e^2 a} \sum_\beta (L_{11}^{-1})_{\alpha\beta} \langle j^c \rangle. \quad (39)$$

Integrating the electric field over the z -coordinate, then yields the voltage across the device, which allows us to extract the resistance-unit-cell-area product via Ohm's law

$$R_n a^2 = \frac{1}{e^2} \sum_{\alpha\beta} (L_{11}^{-1})_{\alpha\beta}. \quad (40)$$

To find the heat current, we substitute the value of the electric field into Eq. (16), which yields

$$\langle j_\alpha^Q \rangle = -\frac{1}{|e|} \sum_{\beta\gamma} L_{21\alpha\beta} (L_{11}^{-1})_{\beta\gamma} \langle j^c \rangle. \quad (41)$$

This is all we need to analyze the Peltier effect of a nanostructure. Note that the heat current generically will have α dependence, and hence will vary from plane to plane (see Fig. 3).

The first question we can ask is how much heat is lost or gained by the reservoir that is attached to the device to maintain isothermal conditions. This is determined by the ratio of the difference in the heat current at the right and the heat current at the left to the charge current. In equations,

$$\begin{aligned} \frac{\Delta \langle j^Q \rangle}{\langle j^c \rangle} &= \frac{\langle j_R^Q \rangle - \langle j_L^Q \rangle}{\langle j^c \rangle} \\ &= -\frac{1}{|e|} \sum_{\beta\gamma} (L_{21R\beta} - L_{21L\beta}) (L_{11}^{-1})_{\beta\gamma}. \end{aligned} \quad (42)$$

This would measure the net cooling or heating of the reservoir by the device as the charge current flows. Similarly, we could measure the average heat flow carried through the device

$$\frac{\langle j_{ave}^Q \rangle}{\langle j^c \rangle} = -\frac{1}{|e|} \frac{1}{N} \sum_{\alpha\beta\gamma} L_{21\alpha\beta} (L_{11}^{-1})_{\beta\gamma}, \quad (43)$$

where N is the number of terms taken in the summation over the index α . This expression is analogous to the bulk Peltier effect, which measures the ratio of the heat to charge current flows (which are independent of position in a bulk system in linear response).

Next we examine the Seebeck effect and a thermal conductivity experiment. In both cases we work with an open circuit, so the total charge current vanishes $\langle j^c \rangle = 0$.

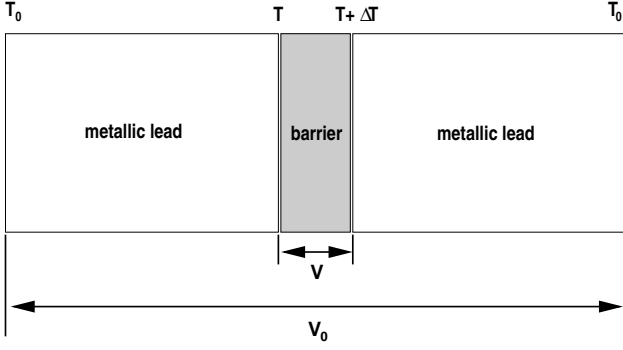


FIG. 4: Schematic diagram for how to measure the (relative) Seebeck effect. The metallic leads are composed of the same material, and a voltage probe is placed across the two ends which both are fixed at a temperature of T_0 . The voltage across those probes is V_0 . Since heat current will flow across the voltmeter if both ends are not at the same temperature, there is no way to directly measure the desired voltage V . But, since the change in voltage in the metallic lead in going from T_0 to T on the left hand side is exactly canceled by the change in voltage in going from T to T_0 on the right hand side, we find the difference between the voltage V and V_0 is just equal to the Seebeck coefficient of the metallic lead multiplied by ΔT . Hence, since a measurement uses V_0 instead of V , the Seebeck coefficient of the barrier is measured *relative to* the Seebeck coefficient of the metallic lead.

The Seebeck measurement is subtle, because we don't want to measure the voltage difference with probes at different temperatures, because there will be a contribution from the $\nabla T d\mu/dT$ terms to the voltage drop (and there may be a thermal link allowing heat to flow through the voltage probe). An actual experiment uses thermocouple probes, where one end of the probe is placed on the sample, and the other is placed in a constant T_0 bath. Two probes are needed to measure the voltage change and the temperature at two points along the sample. The net thermopower is measured relative to the thermopower of the metal used in one of the legs of the thermocouple (typically copper). For details, see Refs. 30 and 31; a simpler schematic picture of this issue is shown in Fig. 4. Alternatively, we can imagine the lead to the left placed in a bath at temperature T_0 , the interface plane on the left held at temperature T , the interface on the right held at temperature $T + \Delta T$, and the lead to the right held at temperature T_0 . The net effect on our analysis, if we assume the thermopower of copper can be neglected (or of the ballistic lead in the alternative picture), is that we neglect the $d\mu_\alpha/dT$ terms in our analysis (because the chemical potential at the probes is at a constant temperature when the potential difference is measured). With these caveats in mind, using Eq. (15), we find

$$E_\alpha = -\frac{1}{a|e|T} \sum_{\beta\gamma} (L_{11}^{-1})_{\alpha\beta} L_{12\beta\gamma} (T_{\gamma+1} - T_\gamma). \quad (44)$$

Multiplying by a and summing over α yields the voltage

drop across the device. We also need the temperature profile. Substituting Eq. (44) into Eq. (16), and noting that the heat current is conserved if the device is isolated and in the steady state (implying heat cannot be transferred out of any plane, recall that the Joule heating is a nonlinear effect) because the system develops a temperature profile so that the heat current is conserved through the device. In this case, we can evaluate the temperature profile, which satisfies

$$T_{\alpha+1} - T_\alpha = -T \sum_{\beta} (M^{-1})_{\alpha\beta} \langle j^Q \rangle, \quad (45)$$

with the matrix M defined to be

$$M_{\alpha\beta} = L_{22\alpha\beta} - \sum_{\gamma\delta} L_{21\alpha\gamma} (L_{11}^{-1})_{\gamma\delta} L_{12\delta\beta}. \quad (46)$$

Now we can sum Eq. (45) over α to get the temperature difference over the device. Hence the Seebeck effect becomes

$$\frac{\Delta V}{\Delta T} = -\frac{1}{|e|T} \frac{\sum_{\alpha\beta\gamma\delta} (L_{11}^{-1})_{\alpha\beta} L_{12\beta\gamma} M_{\gamma\delta}^{-1}}{\sum_{\alpha\beta} M_{\alpha\beta}^{-1}}. \quad (47)$$

Note that this is not equal to $1/T$ times the Peltier coefficient as in the bulk [see Eqs. (42) and (43)]. Instead, we have a weighting of the L_{12} to L_{11} ratio by the matrix M , which is related to the thermal conductivity. This factor cancels in the bulk, where the M matrix depends on the difference of the spatial coordinates, and the $\mathbf{q} = 0$ response is independent of M because the common factor in the Fourier transform will cancel out (as can easily be proved by invoking the convolution theorem). If we do not measure ΔV via thermocouples at constant T , then the ΔV term is modified by a contribution from $d\mu_\alpha/dT$. We do not discuss that modification here, because it is not normally a technique used in measurements¹⁴.

The thermal conductance is evaluated in a similar way, but does not require any subtlety in the measurement. We also work in an open circuit, and the heat current is conserved, because we isolate the system. Now we measure the ratio of the heat current to the temperature difference to find that the thermal conductance per unit area K satisfies

$$K = -\frac{\langle j^Q \rangle}{\Delta T} = \frac{1}{T \sum_{\alpha\beta} (M^{-1})_{\alpha\beta}}, \quad (48)$$

and the thermal resistance-area product becomes

$$R_{\text{th}} a^2 = T \sum_{\alpha\beta} (M^{-1})_{\alpha\beta}. \quad (49)$$

Given all of the phenomenological parameters that enter into the transport of a nanostructure, we are now in a position to be able to evaluate things like the efficiency of a refrigerator, or of a power generator (this requires evaluating heat flow while charge current is flowing, and

is more complex than the cases considered here). The final equations that result are quite complicated, and will not be shown here. Note that it is necessary to perform such an exercise here, because in these nanostructure devices, the thermoelectric cooling or power generation is not determined solely by the bulk figure of merit of the constituent pieces. When quantum effects enter due to nanoscale structures, the situation is more complicated. But one can define an effective figure-of-merit by constructing an effective Lorenz number from the ratio of the thermal to the charge resistance and then evaluate an effective figure-of-merit from the Seebeck coefficient and the effective Lorenz number. Even if this is done, it is not the same as the calculation of the efficiency of a real device, which simply is more complicated.

V. CONCLUSIONS

In this work we have shown how to derive the formalism for evaluating the electronic contribution to the charge and thermal transport of a strongly correlated nanostructure by determining the appropriate Kubo formulas for the transport coefficients. This analysis requires us to properly determine the local current operators, which we do via a heuristic argument. Using these specific local current operators allows us to show that the Kubo formulas for the various heat transport coefficients are related by a generalization of the Jonson-Mahan theorem to inhomogeneous systems. We also describe how nanostructures that will be used for heat transport must have an associated electronic charge reconstruction, and we sketched how to solve for that reconstruction using the DMFT approximation in the nanostructure. We illustrated our results for models described by the Hubbard model, the Falicov-Kimball model, and the periodic Anderson model, but they should hold for any model that involves only local interactions.

It will be interesting to now solve some numerical problems and investigate the thermal transport coefficients for these systems. Devices of particular interest are those that have strongly correlated electrons, such as systems with a Mott insulator, a doped Mott insulator, or Kondo metals in them. Solving such problems is easiest to do for the Falicov-Kimball model because it is the easiest model to solve numerically, but it should be feasible to investigate the Hubbard model and the periodic Anderson model as well using numerical renormalization group techniques, or quantum Monte Carlo plus maximum entropy analytic continuations. Such work will be presented elsewhere.

APPENDIX A: VANISHING OF CURRENTS FOR AN EQUILIBRIUM ELECTRONIC CHARGE RECONSTRUCTION

We prove that the charge and heat current expectation values vanish in equilibrium when there is an electronic charge reconstruction, in the case where the self-energy is local. The result should also hold for the nonlocal case, by purely physical reasons, but we are not aware of a simple way to prove this result in the general case.

Because the multilayered system is translationally invariant in each plane, we can use a mixed basis, where we have a two-dimensional momentum describing the planar degrees of freedom, and we use real-space to describe the inhomogeneous z -direction¹⁵. Then, if we assume the self-energy is a local function Σ_α , that can vary from one plane to another, we have the local Green's function satisfies¹⁸

$$G_{\alpha\alpha}(\mathbf{k}^\parallel, \omega) = 1/\{L_\alpha(\mathbf{k}^\parallel, \omega) + R_\alpha(\mathbf{k}^\parallel, \omega) - [\omega + \mu - V_\alpha + \Delta E_{F\alpha} - \Sigma_\alpha(\omega) - \epsilon_{\alpha\mathbf{k}^\parallel}^\parallel]\} \quad (\text{A1})$$

where $\epsilon_{\alpha\mathbf{k}^\parallel}^\parallel$ is the two-dimensional (planar) bandstructure on plane α , and the left L_α and right R_α functions are defined below. The local Green's function on each plane is then found by summing over the two-dimensional momenta, which can be replaced by an integral over the two-dimensional density of states:

$$G_{\alpha\alpha}(\omega) = \int d\epsilon_\alpha^\parallel \rho^{2d}(\epsilon_\alpha^\parallel) G_{\alpha\alpha}(\epsilon_\alpha^\parallel, \omega), \quad (\text{A2})$$

The left function is defined to be

$$L_{\alpha-n}(\mathbf{k}^\parallel, \omega) = -\frac{G_{\alpha\alpha-n+1}(\mathbf{k}^\parallel, \omega)t_{\alpha-n+1\alpha-n}^\perp}{G_{\alpha\alpha-n}(\mathbf{k}^\parallel, \omega)} \quad (\text{A3})$$

and it satisfies the recurrence relation

$$L_{\alpha-n}(\mathbf{k}^\parallel, \omega) = \omega + \mu - V_\alpha + \Delta E_{F\alpha} - \Sigma_{\alpha-n}(\omega) - \epsilon_{\alpha-n\mathbf{k}^\parallel}^\parallel - \frac{t_{\alpha-n\alpha-n-1}^\perp t_{\alpha-n-1\alpha-n}^\perp}{L_{\alpha-n-1}(\mathbf{k}^\parallel, \omega)}. \quad (\text{A4})$$

We solve the recurrence relation by starting with the result for $L_{-\infty}$, and then iterating Eq. (A4). In a similar fashion, we define a right function and a recurrence relation to the right, with the right function satisfying

$$R_{\alpha+n}(\mathbf{k}^\parallel, \omega) = -\frac{G_{\alpha\alpha+n-1}(\mathbf{k}^\parallel, \omega)t_{\alpha+n-1\alpha+n}^\perp}{G_{\alpha\alpha+n}(\mathbf{k}^\parallel, \omega)} \quad (\text{A5})$$

and the recurrence relation being

$$R_{\alpha+n}(\mathbf{k}^\parallel, \omega) = \omega + \mu - V_\alpha + \Delta E_{F\alpha} - \Sigma_{\alpha+n}(\omega) - \epsilon_{\alpha+n\mathbf{k}^\parallel}^\parallel - \frac{t_{\alpha+n\alpha+n+1}^\perp t_{\alpha+n+1\alpha+n}^\perp}{R_{\alpha+n+1}(\mathbf{k}^\parallel, \omega)}. \quad (\text{A6})$$

We solve the right recurrence relation by starting with the result for R_∞ , and then iterating Eq. (A6).

In order to determine the current, we need to examine the off-diagonal, nearest neighbor Green's functions, which satisfy

$$G_{\alpha+1\alpha}(\mathbf{k}^{\parallel}, \omega) = -\frac{G_{\alpha+1\alpha+1}(\mathbf{k}^{\parallel}, \omega)t_{\alpha+1\alpha}^{\perp}}{L_{\alpha}(\mathbf{k}^{\parallel}, \omega)}, \quad (\text{A7})$$

and

$$G_{\alpha\alpha+1}(\mathbf{k}^{\parallel}, \omega) = -\frac{G_{\alpha\alpha}(\mathbf{k}^{\parallel}, \omega)t_{\alpha\alpha+1}^{\perp}}{R_{\alpha+1}(\mathbf{k}^{\parallel}, \omega)}. \quad (\text{A8})$$

Using the recursion relations for the Green's functions and for the R and L functions allows us to express the result for the Green's functions in terms of $R_{\alpha+1}$ and L_{α} . Hence, we find

$$\begin{aligned} G_{\alpha\alpha+1}(\mathbf{k}^{\parallel}, \omega) &= G_{\alpha+1\alpha}(\mathbf{k}^{\parallel}, \omega) \\ &= \frac{1}{L_{\alpha}(\mathbf{k}^{\parallel}, \omega)R_{\alpha+1}(\mathbf{k}^{\parallel}, \omega) - t_{\alpha\alpha+1}^{\perp}t_{\alpha+1\alpha}^{\perp}}. \end{aligned} \quad (\text{A9})$$

Now, we are ready to show the expectation value of the number current operator vanishes. We can evaluate the expectation value of the number current operator in Eq. (18) by using the Green's functions we have been describing above. One finds

$$\langle j_{\alpha} \rangle = at_{\alpha\alpha+1}^{\perp} \int d\omega \sum_{\mathbf{k}^{\parallel}} [G_{\alpha+1\alpha}(\mathbf{k}^{\parallel}, \omega) - G_{\alpha\alpha+1}(\mathbf{k}^{\parallel}, \omega)] = 0, \quad (\text{A10})$$

which vanishes because the two Green's functions are identical in value. Note that this vanishing of the current holds for arbitrary size electronic charge reconstruction, because it does not involve any linear-response assumption. Similarly, since the heat-current operator is related

to the number current operator by a derivative with respect to time, and that derivative analytically continues to an extra power of frequency in the integral over frequency, we also have that the heat-current operator expectation value vanishes, because it involves adding an extra power of frequency into the above integrals. This then completes the proof that the electronic charge reconstruction does not have any currents flowing through it, so the electric fields that enter the linear-response formalism are the external fields only.

APPENDIX B: ANALYTIC CONTINUATION OF THE FOUR-TIME RESPONSE FUNCTION NEEDED FOR THE GENERAL JONSON-MAHAN THEOREM PROOF

We can restrict ourselves to the case $\tau_1 > \tau_2 > \tau_3 > \tau_4$ without loss of generality, because that is the ordering needed to get the relevant correlation functions in Eqs. (29). First of all, let us introduce a four-time correlation function (in real time) defined by

$$\begin{aligned} I_{ABCD}(t_1, t_2, t_3, t_4) &= I_{ABCD}(t_1 - t, t_2 - t, t_3 - t, t_4 - t) \\ &= \langle A(t_1)B(t_2)C(t_3)D(t_4) \rangle, \end{aligned} \quad (\text{B1})$$

where all operators are written in the Heisenberg representation $\mathcal{O}(t) = \exp[i(\mathcal{H} - \mu\mathcal{N})t]\mathcal{O}\exp[-i(\mathcal{H} - \mu\mathcal{N})t]$ ($\hbar = 1$). Its Fourier transform gives a four-time spectral density (with the constraint $\omega_1 + \omega_2 + \omega_3 + \omega_4 = 0$ due to time-translation invariance of equilibrium correlation functions)

$$\begin{aligned} I_{ABCD}(\omega_1, \omega_2, \omega_3, \omega_4) &= \int_{-\infty}^{+\infty} \frac{dt_1}{2\pi} \int_{-\infty}^{+\infty} \frac{dt_2}{2\pi} \int_{-\infty}^{+\infty} \frac{dt_3}{2\pi} \exp[i\omega_1 t_1 + i\omega_2 t_2 + i\omega_3 t_3 + i\omega_4 t_4] I_{ABCD}(t_1, t_2, t_3, t_4) \\ &= \frac{1}{\mathcal{Z}} \sum_{ilfp} e^{-\beta\varepsilon_i} A_{il} B_{lf} C_{fp} D_{pi} \delta(\varepsilon_{il} + \omega_1) \delta(\varepsilon_{lf} + \omega_2) \delta(\varepsilon_{fp} + \omega_3), \end{aligned} \quad (\text{B2})$$

where ε_i is the energy eigenvalue of the quantum many-body state $|i\rangle$ (*i. e.*, the eigenvalue of the operator $\mathcal{H} - \mu\mathcal{N}$), ε_{il} satisfies $\varepsilon_{il} = \varepsilon_i - \varepsilon_l$, $\mathcal{O}_{il} = \langle i|\mathcal{O}|l\rangle$ is the matrix element of the operator \mathcal{O} between the states i and l , and $\mathcal{Z} = \sum_i e^{-\beta\varepsilon_i}$ is the partition function. The second line in Eq. (B2) follows from the Lehmann representation by inserting appropriate sets of complete states. The spectral density satisfies the following cyclic permutation identities

$$I_{ABCD}(\omega_1, \omega_2, \omega_3, \omega_4) = I_{BCDA}(\omega_2, \omega_3, \omega_4, \omega_1)e^{\beta\omega_1} = I_{CDAB}(\omega_3, \omega_4, \omega_1, \omega_2)e^{\beta(\omega_1 + \omega_2)} = I_{DABC}(\omega_4, \omega_1, \omega_2, \omega_3)e^{-\beta\omega_4} \quad (\text{B3})$$

and transforms under Hermitian conjugation as

$$I_{ABCD}(\omega_1, \omega_2, \omega_3, \omega_4) = [I_{D^{\dagger}C^{\dagger}B^{\dagger}A^{\dagger}}(-\omega_4, -\omega_3, -\omega_2, -\omega_1)]^*, \quad (\text{B4})$$

with the dagger indicating Hermitian conjugation of the associated operator. Now, the generalized function in Eq. (28) can be defined for $\tau_1 > \tau_2 > \tau_3 > \tau_4$ in terms of a generalized spectral density as

$$F_{\alpha\beta}(\tau_1 > \tau_2 > \tau_3 > \tau_4) = \int_{-\infty}^{+\infty} d\omega_1 \int_{-\infty}^{+\infty} d\omega_2 \int_{-\infty}^{+\infty} d\omega_3 I_{\alpha\beta}(\omega_1, \omega_2, \omega_3, \omega_4) \exp[-\omega_1\tau_1 - \omega_2\tau_2 - \omega_3\tau_3 - \omega_4\tau_4], \quad (\text{B5})$$

where we introduce the total spectral density in terms of the partial one in Eq. (B2)

$$I_{\alpha\beta}(\omega_1, \omega_2, \omega_3, \omega_4) = -a^2 t_{\alpha\alpha+1}^\perp t_{\beta\beta+1}^\perp \sum_{i \in \text{plane}} \sum_{j \in \text{plane}} \left[I_{c_{\alpha+1i}^\dagger c_{\alpha i} c_{\beta+1j}^\dagger c_{\beta j}}(\omega_1, \omega_2, \omega_3, \omega_4) + I_{c_{\alpha i}^\dagger c_{\alpha+1i} c_{\beta j}^\dagger c_{\beta+1j}}(\omega_1, \omega_2, \omega_3, \omega_4) \right. \\ \left. - I_{c_{\alpha+1i}^\dagger c_{\alpha i} c_{\beta j}^\dagger c_{\beta+1j}}(\omega_1, \omega_2, \omega_3, \omega_4) - I_{c_{\alpha i}^\dagger c_{\alpha+1i} c_{\beta+1j}^\dagger c_{\beta j}}(\omega_1, \omega_2, \omega_3, \omega_4) \right]. \quad (\text{B6})$$

Next, we can calculate the polarization operators in Eq. (29) by taking the appropriate limits and derivatives. Namely,

$$\bar{L}_{ij\alpha\beta}(i\nu) = \int_{-\infty}^{+\infty} d\omega_1 \int_{-\infty}^{+\infty} d\omega_2 \int_{-\infty}^{+\infty} d\omega_3 I_{\alpha\beta}(\omega_1, \omega_2, \omega_3, \omega_4) \frac{e^{-\beta(\omega_1+\omega_2)} - 1}{i\nu + \omega_1 - \omega_2} \begin{cases} 1 & \text{for } ij = 11 \\ \frac{1}{2}(\omega_4 - \omega_3) & \text{for } ij = 12 \\ \frac{1}{2}(\omega_2 - \omega_1) & \text{for } ij = 21 \\ \frac{1}{4}(\omega_2 - \omega_1)(\omega_4 - \omega_3) & \text{for } ij = 22 \end{cases}. \quad (\text{B7})$$

Here, one notes that $\omega_4 = -\omega_1 - \omega_2 - \omega_3$ due to the constraint. Then we replace $i\nu$ by $\nu + i0^+$ and construct the transport coefficients on the real axis. Finally we take the limit $\nu \rightarrow 0$ to obtain the dc response

$$L_{ij\alpha\beta} = \lim_{\nu \rightarrow 0} \frac{1}{2i\nu} [\bar{L}_{ij\alpha\beta}(\nu + i0^+) - \bar{L}_{ij\alpha\beta}(\nu - i0^+)] = \pi\beta \int_{-\infty}^{+\infty} d\omega_2 \int_{-\infty}^{+\infty} d\omega_4 I_{\alpha\beta}(-\omega_2, \omega_2, -\omega_4, \omega_4) \omega_2^{i-1} \omega_4^{j-1}, \quad (\text{B8})$$

where, by using the identities in Eqs. (B3) and (B4), the spectral density in Eq. (B6) can be reduced to the following expression

$$I_{\alpha\beta}(-\omega_2, \omega_2, -\omega_4, \omega_4) = -2a^2 t_{\alpha\alpha+1}^\perp t_{\beta\beta+1}^\perp \sum_{i \in \text{plane}} \sum_{j \in \text{plane}} \text{Re} \left[I_{c_{\alpha+1i}^\dagger c_{\alpha i} c_{\beta+1j}^\dagger c_{\beta j}}(-\omega_2, \omega_2, -\omega_4, \omega_4) \right. \\ \left. - I_{c_{\alpha+1i}^\dagger c_{\alpha i} c_{\beta j}^\dagger c_{\beta+1j}}(-\omega_2, \omega_2, -\omega_4, \omega_4) \right]. \quad (\text{B9})$$

Eqs. (B8) and (B9) are the generalization of the Jonson-Mahan theorem to nanostructures; the integrands for the charge-charge, heat-charge, charge-heat, and heat-heat current operator correlation functions are all related by powers of frequency. One can also check that the Onsager reciprocal relation holds, where L_{12} is equal to L_{21} . This follows by using the symmetry relations, and then interchanging the dummy integration variables ω_2 and ω_4 .

In the case where we neglect vertex corrections, the spectral densities in Eq. (B9) are equal to

$$I_{c_{\alpha+1i}^\dagger c_{\alpha i} c_{\beta+1j}^\dagger c_{\beta j}}(-\omega_2, \omega_2, -\omega_4, \omega_4) \\ = I_{c_{\alpha i} c_{\beta+1j}^\dagger c_{\beta j} c_{\alpha+1i}^\dagger}(\omega_2, -\omega_4, \omega_4, \omega_2) e^{\beta\omega_4} \\ = \bar{I}_{c_{\beta j} c_{\alpha+1i}^\dagger}(\omega_4) \bar{I}_{c_{\alpha i} c_{\beta+1j}^\dagger}(\omega_4) e^{\beta\omega_4} \delta(\omega_2 - \omega_4) \quad (\text{B10})$$

and

$$I_{c_{\alpha+1i}^\dagger c_{\alpha i} c_{\beta j}^\dagger c_{\beta+1j}}(-\omega_2, \omega_2, -\omega_4, \omega_4) \\ = I_{c_{\alpha i} c_{\beta j}^\dagger c_{\beta+1j} c_{\alpha+1i}^\dagger}(\omega_2, -\omega_4, \omega_4, -\omega_2) e^{\beta\omega_4} \\ = \bar{I}_{c_{\beta+1j} c_{\alpha+1i}^\dagger}(\omega_4) \bar{I}_{c_{\alpha i} c_{\beta j}^\dagger}(\omega_4) e^{\beta\omega_4} \delta(\omega_2 - \omega_4), \quad (\text{B11})$$

respectively, where

$$\bar{I}_{AB}(\omega) = -\frac{1}{\pi} f(\omega) \text{Im} G_{BA}(\omega) \quad (\text{B12})$$

are the single-particle spectral densities, and we obtain the same result as in Eq. (38). In the general case, when vertex corrections are included, one can find the spectral densities in Eq. (B2) from the multitime temperature (Matsubara) Green's function in Eq. (28) by employing spectral relations for the multitime correlation functions³². The full derivation is complex and lengthy. In the end it provides no new information with relation to the Jonson-Mahan theorem, only an explicit formula

for the charge conductivity matrix. Hence, we do not go through the derivation here.

ACKNOWLEDGMENTS

We are grateful to P. Allen, G. Mahan, and L. Sham for useful discussions. Support from the N. S. F. un-

der grant number DMR-0210717 is acknowledged. This publication is also based on work supported by Award No. UKP2-2697-LV-06 of the U.S. Civilian Research & Development Foundation (CRDF).

-
- * Electronic address: freericks@physics.georgetown.edu;
URL: <http://www.physics.georgetown.edu/~jkf/index.html>
- † Electronic address: zlatić@ifs.hr
- ‡ Electronic address: ashv@icmp.lviv.ua;
URL: <http://ph.icmp.lviv.ua/~ashv/>
- ¹ M. Rontani and L. J. Sham, Appl. Phys. Lett. **77**, 3033 (2001).
 - ² M. Bartkowiak and G. D. Mahan, in *Semiconductors and semimetals* Vol. **71**, (Academic press, new York, 2001), p. 245.
 - ³ M. Jonson and G. D. Mahan, Phys. Rev. B **21**, 4223 (1980).
 - ⁴ M. Jonson and G. D. Mahan, Phys. Rev. B **42**, 9350 (1990).
 - ⁵ L. D. Hicks and M. S. Dresselhaus, Phys. Rev. B **47**, 12727 (1993).
 - ⁶ R. Ventkatasubramanian, E. Silvola, T. Colpitts, and B. O'Quinn, Nature **413**, 597 (2001).
 - ⁷ J. Hubbard, Proc. R. Soc. (London) Ser. A **276**, 238 (1963).
 - ⁸ L. M. Falicov and J. C. Kimball, Phys. Rev. Lett. **22**, 997 (1969).
 - ⁹ P. W. Anderson, Phys. Rev. **124**, 41 (1961).
 - ¹⁰ W. Schottky, Phys. Z. **41**, 570 (1940).
 - ¹¹ B. K. Nikolić, J. K., Freericks and P. Miller Phys. Rev. B **65**, 064529 (2002).
 - ¹² S. Okamoto and A. J. Millis, Nature **428**, 630 (2004); Phys. Rev. B **70**, 241104(R) (2004).
 - ¹³ W.-C. Lee and A. H. MacDonald, Phys. Rev. B **74**, 075106 (2006).
 - ¹⁴ J. Cai and G. D. Mahan, Phys. Rev. B **74**, 075201 (2006).
 - ¹⁵ M. Potthoff and W. Nolting, Phys. Rev. B **59**, 2549 (1999).
 - ¹⁶ P. Ewald, Ann. Phys. (Leipzig) **64**, 253 (1921).
 - ¹⁷ E. N. Economou, *Green's functions in quantum physics* (Springer-Verlag, Berlin, 1983).
 - ¹⁸ J. K. Freericks, Appl. Phys. Lett. **84**, 1383 (2004); Phys. Rev. B **70**, 195342 (2004).
 - ¹⁹ L. Chen and J. K. Freericks, *unpublished*.
 - ²⁰ L. Onsager, Phys. Rev. **37**, 405 (1931); Phys. Rev. **38**, 2265 (1931).
 - ²¹ A. Fick, Poggendorff's Ann. Phys. u. Chemie **94**, 59 (1855).
 - ²² A. Einstein, Ann. Phys. (Leipzig) **17**, 549 (1905).
 - ²³ W. H. Nernst, Z. Phys. Chem. **4**, 129 (1889).
 - ²⁴ M. von Smoluchowski, Ann. Phys. (Leipzig) **21**, 756 (1906).
 - ²⁵ J. M. Luttinger, Phys. Rev. **135**, A1505 (1964).
 - ²⁶ G. S. Ohm, *The Galvanic current investigated mathematically* (J. G. F. Kniestädt, Berlin, 1827).
 - ²⁷ J. C. A. Peltier, Ann. Chim. Phys. **56**, 371 (1834).
 - ²⁸ J. B. J. Fourier, *Theorie analytique de la chaleur* (Firman, Didot, Paris, 1822); English translation: *The analytic theory of heat*, translated by A. Freeman (Cambridge University Press, Cambridge, 1878).
 - ²⁹ T. J. Seebeck, Abhandlung der Deutschen Akademie der Wissenschaft zu Berlin, 265 (1823).
 - ³⁰ C. A. Domenicali, Rev. Mod. Phys. **26**, 237 (1954).
 - ³¹ G. S. Nolas, J. Sharp and J. Goldsmid *Thermoelectrics: Basic Principles and New Materials Developments* (Springer-Verlag, Berlin, 2001).
 - ³² A. M. Shvaika, Condens. Matter Phys. **9**, XXX (2006) (in press); *preprint arXiv:cond-mat/0604621*.